Bulletin of the Seismological Society of America, Vol. 86, No. 2, pp. 519–523, April 1996

Short Notes

The Accuracy of Soil Response Estimates Using Soil-to-Rock Spectral Ratios

by Igor A. Beresnev and Kuo-Liang Wen

Abstract Spectral ratios between soft soil and reference rock sites are often used to predict the sedimentary site response to earthquakes. However, their relationship with the genuine site-specific amplification function is often unclear. We compare the soil-to-rock spectral ratios between the stations that are 3.3 km apart with the "genuine" response given by the ratios between the surface and 17 and 47 m downhole. Data from the SMART1 array in Taiwan are used. The "weak" and "strong" motion records are addressed separately to allow for nonlinear soil response. The soil-to-rock spectral ratios are nearly identical to the "true" amplification at the frequencies from 1 to 10 Hz, if the finite depth of the borehole is taken into account. They correctly capture the strong-motion deamplification effect. However, the soil-to-rock spectral ratios are roughly 1.4 times more uncertain than surface-to-47-m ratios. In summary, the soil-to-rock spectral ratios can be considered as the reliable estimates of the real site response.

Introduction

The amplification of seismic waves by soft near-surface deposits is a well-known cause of structural damage during earthquakes (e.g., Çelebi *et al.,* 1987). Obtaining reliable estimates of the site-specific soil amplification function is thus an important engineering task.

Empirical estimate of the transfer function of sediments in its exact form requires the knowledge of the output signal recorded at surface, as well as the input motion at the base of the sediments. The latter is virtually never known. An alternative method, dating back to Borcherdt (1970), uses the spectral ratio between the sedimentary site and the nearby bedrock reference site. However, the assumption that the seismic signal recorded at the rock site represents an undisturbed input motion is never totally right. Also, differential source and path effects between the soil and the reference stations are not eliminated by dividing the spectra.

Given these problems, the accuracy of site-response estimates obtained in many practical situations using the soil-to-rock spectral ratios is simply not known. Their correlation with the true response needs special attention. The purpose of this work is to carry out such an investigation for a typical practical situation.

We assume that the "true" site response can be obtained from the vertical strong motion arrays by dividing the surface by the downhole spectra. If the records at an adjacent basement outcrop are available, the true transfer function can be used to validate the accuracy of the site response provided by the surface-to-rock spectral ratio.

SMART1 and LSST Strong Motion Arrays

We use the records of the SMART1 surface accelerograph array that was deployed in northeastern Taiwan in 1980 and recorded local strong-motion data until 1990 (Abrahamson *et al.,* 1987). All but one of the SMART1 stations were positioned on the recent alluvial plain of the Lanyang river with uniform site conditions. Station E-02 was installed on a basement slate outcrop (Fig. 1). Figure 2 depicts a north–south cross section across the array (Wen and Yeh, 1984). The surficial layer consists of sandy silt with some gravel and is geotechnically classified as "deep cohesionless soil." Basement rock is the Miocene Lushan formation. Its exposure to the south of the profile in Figure 2 has been occupied by the E-02 reference station.

In October 1985, a vertical accelerograph array was installed in the south-west quadrant of the SMART1 array as part of the LSST (Lotung large-scale seismic test) project, with instruments placed at surface and at depths of 6, 11, 17, and 47 m. The distance between the vertical array and station E-02 is 3.3 km. Low-strain *S*-wave velocities at the borehole are given in Figure 3 (Wen, 1994).

The SMART1 data were digitized as 12-bit words at 100 samples per second. The preprocessing included baseline subtraction and high- and low-pass filtering with cut frequencies of 0.1 and 25 Hz, respectively. The pre-event memory was set to 2.5 sec. The downhole array was equipped with Kinemetrics FBA-13DH sensors, and the data

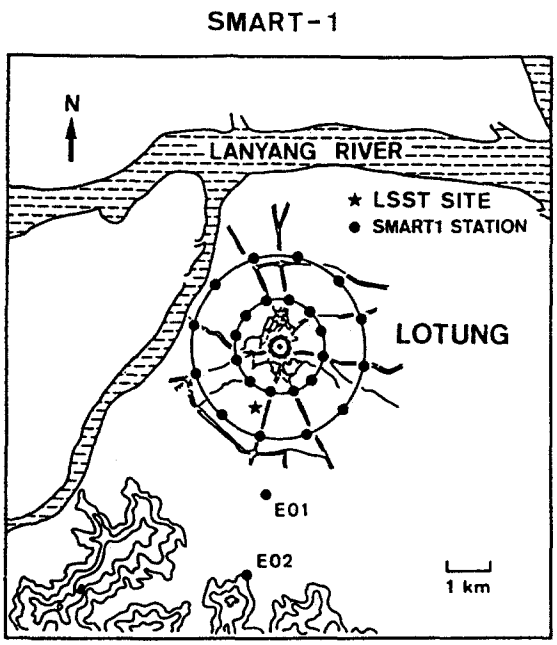

Figure 1. Location of the bedrock station E-02 and the downhole accelerograph array (star) within the SMART1 array. Circles stand for the SMART1 stations.

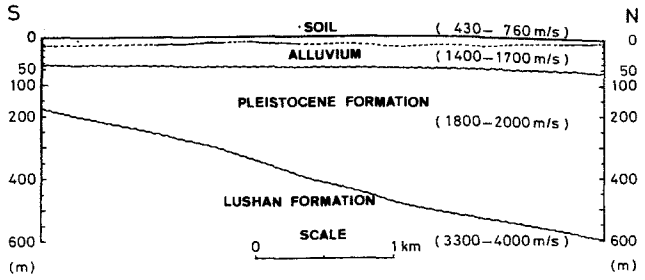

Figure 2. North–south profile across the SMART1 array with the range of *P*-wave velocities.

were digitized as 12-bit words at 200 samples per second. The pre-event memory was 5.1 sec. The filter cut frequencies were 0.1 and 50 Hz.

The combination of the SMART1 and the LSST records enables us to obtain both the "exact" response at the LSST site using borehole data and the response relative to the rock station. The parameters of the seismic events jointly recorded by the LSST array and the E-02 station are summarized in Table 1. Their epicenters are shown in Figure 4. In the following section, we address the borehole records at surface, 17 m, and 47 m only. Table 1 also shows that the instrument at 47 m did not operate after earthquake 11 had been recorded. We will compare the surface-to-17-m and the surface-to-47-m spectral ratios with those calculated between the surface and the rock site. Only the response to shear waves is considered.

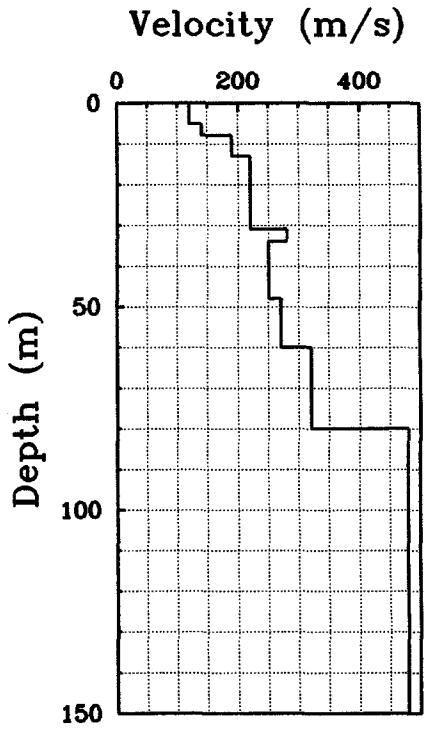

Figure 3. Shear-wave velocity profile at the LSST site.

Table 1
Selected Events

Event*	Date	Depth (km)	M_L	Δ† (km)	PHA‡ at Rock Site (cm/sec²)	PHA‡ at Borehole (cm/sec²) Surface	17 m	47 m
2	26/10/85	1.7	4.7	28.6	44.9	60.4	24.0	—
4	16/01/86	10.2	6.1	25.8	197.5	258.0	—	177.9
7	20/05/86	15.8	6.2	68.1	186.0	203.7	100.0	96.9
8	20/05/86	21.8	5.8	72.6	49.1	34.3	14.9	14.2
11	17/07/86	2.0	4.3	6.4	65.6	101.8	57.1	60.5
12	30/07/86	1.6	5.8	5.5	245.9	186.7	186.0	—
14	30/07/86	2.3	4.3	5.2	20.8	49.4	28.7	—
16	14/11/86	15.0	6.5	76.0	139.8	167.2	85.2	—
25	10/11/87	34.4	4.9	43.8	56.5	78.3	40.9	—

*Event number in LSST array classification.
†Hypocentral distance to downhole array.
‡Peak horizontal acceleration.

Method

We calculate the spectral ratios as follows: (1) a window containing the shear wave is identified; (2) the window is tapered at both ends (at 5% of the length) using a cosine function; (3) the Fourier amplitude spectrum is calculated; (4) the spectrum is smoothed 10 times using a 3-point running Hanning average; (5) two smoothed spectra are divided; (6) the average horizontal spectral ratio is then calculated by summing the squares of the ratios for E–W and N–S components, dividing by two, and taking the square root.

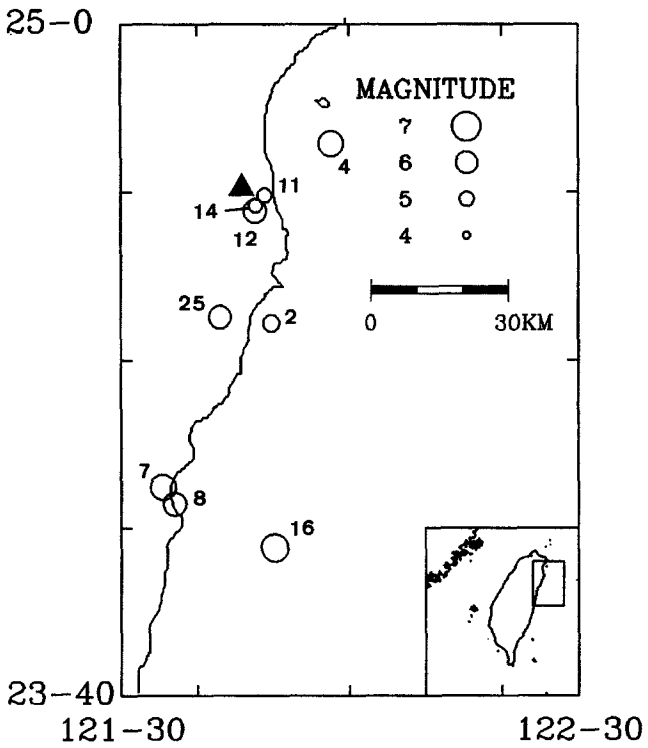

Figure 4. Epicenters of the selected earthquakes (circles). The circle size scales with the magnitude; the triangle stands for the location of the SMART1 array.

The ratio between the borehole and the rock site needs correction for the differential attenuation and geometric spreading effects. This is done using the formula

$$\frac{S_1}{S_2} = \frac{g_1}{g_2}\frac{r_1}{r_2} e^{\pi(r_1 - r_2)f/VQ}, \quad (1)$$

where S_1/S_2 is the corrected response, g_i is the spectrum of the recorded motion, r_i is the hypocentral distance, f is the frequency, V is the shear-wave velocity, and Q is the quality factor (Jarpe *et al.*, 1988). We assume $V = 3.5$ km/sec and $Q = 225 f^{1.1}$, characteristic of northeastern Taiwan (Wang, 1993).

A signal-to-noise ratio (S/N) was estimated from accelerograms having sufficiently long pre-event noise time history, by dividing the smoothed amplitude spectra of the S wave and the pre-event noise. The reliable frequency band, where S/N is greater than 5, is found to be between 1 and 10 Hz. All the results are plotted in this range.

Results

Figure 5 compares the "true" soil amplification function at LSST obtained from the surface-to-47-m spectral ratio (thick line) with the amplification between the same surface instrument and the station E-02. The average curves calculated from the earthquakes in Table 1 are presented together with their standard deviations.

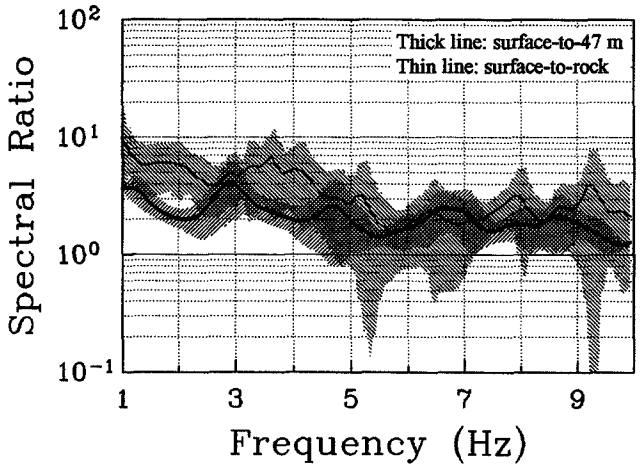

Figure 5. The "true" shear-wave soil amplification function given by the surface-to-47-m spectral ratio (thick line) versus the surface-to-rock spectral ratio (thin line). The shaded bands represent ±1 standard deviation.

It is known that the values of soil amplification can differ considerably for weak and strong ground motion due to nonlinear material behavior (Aki, 1993). Strong-motion deamplification is indeed considerable at the LSST site (Wen *et al.*, 1994; Beresnev *et al.*, 1995). Thus, to reduce the values of standard deviation, the records with significantly different amplitudes should not be mixed to estimate the average amplification. For this reason, we excluded the weakest (according to the peak acceleration at rock site) event 14 from the calculation of the soil-to-rock curve in Figure 5.

Figure 6 similarly compares the surface-to-17-m and surface-to-rock spectral ratios. As seen from Table 1, the higher number of the recordings made by the 17-m accelerometer permits a comparison of the weak- and strong-motion ratios independently. For this purpose, we divided the earthquakes into two groups according to the peak horizontal acceleration (PHA) at the rock site. Events with the PHA of less than 100 cm/sec^2 were attributed to the "weak-motion" class (events 2, 8, 11, 14, and 25), while those with the PHA exceeding 100 cm/sec^2 were classified as "strong motions" (events 4, 7, 12, and 16). Amplifications in weak- and strong-motion groups are shown in Figs. 6a and 6b, respectively.

Discussion

Figure 5 shows that the spectral ratio between the surface and the bedrock gives a reasonably good approximation of the "true" soil amplification function. The curves are almost identical (within the error margin) above the frequency of ~5 Hz, whereas the soil-to-rock ratio overestimates the

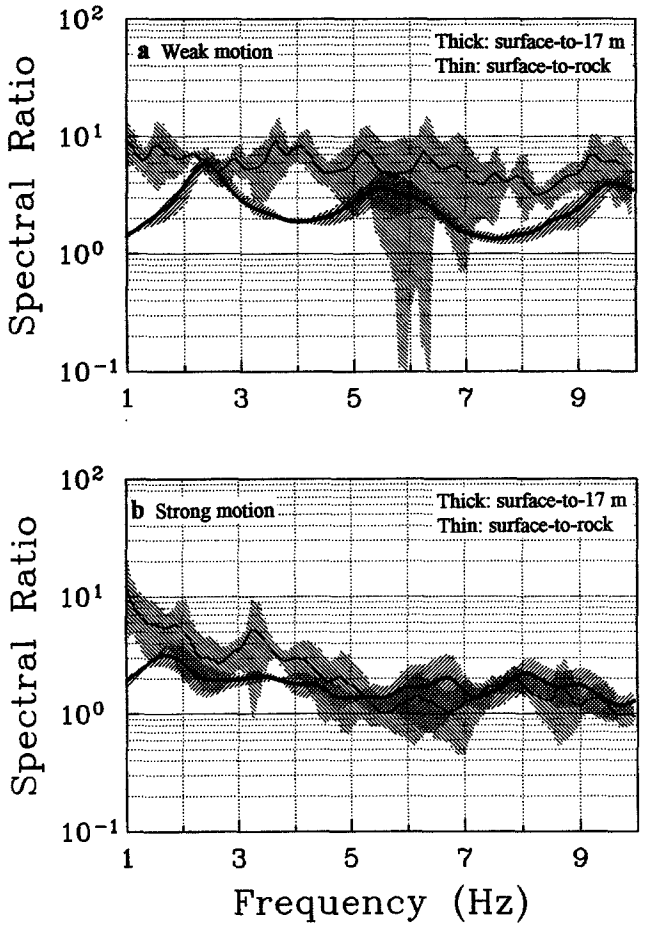

Figure 6. Surface-to-17-m spectral ratios (thick lines) compared with surface-to-rock spectral ratios (thin lines) in (a) weak and (b) strong motion.

"true" response up to a factor of 2.8 at the lower frequencies. However, this apparent disagreement can be explained by the fact that the soil-to-rock ratio characterizes the amplification of seismic waves by the entire sedimentary column below the LSST site, while the "true" amplification function reflects the response of the upper 47 m alone.

We can estimate the contribution to site amplification that would be expected from the Pleistocene stratum that lies between the bottom of the borehole and the base (Fig. 2). Three factors are known to contribute to the total amplification. First, the transmission coefficient at the bottom of a Pleistocene layer is $A' = 2/[(\rho_1 V_1)/(\rho_2 V_2) + 1]$, where ρ is the density and the indexes 1 and 2 stand for the Pleistocene layer and the basement rock, respectively (equation 5.32 and Table 5.2 of Aki and Richards, 1980). Assuming, due to the lack of the data, that the densities are equal, and using the median velocities, we get the amplification due to transmission as $A' = 2/[(1900/3650) + 1] \approx 1.3$. Second, amplification at the resonance frequencies equals $A'' = (\rho_2 V_2)/(\rho_1 V_1)$ (Murphy *et al.*, 1971 p. 114), or, under the same assumptions, $A'' = 3650/1900 \approx 1.9$. Finally, the vertical impedance gradient in the Pleistocene layer may cause an amplification by a factor of $A''' = [(\rho_B V_B)/(\rho_T V_T)]^{1/2}$, where impedances are taken at the bottom (index B) and the top (index T) of the layer (Shearer and Orcutt, 1987 p. 1172). Suppose that the velocity varies gradually from 2000 m/sec at the bottom to 1800 m/sec at the top (Fig. 2). Then $A''' = (2000/1800)^{1/2} \approx 1.1$. Then, the maximum amplification that could be expected from the Pleistocene layer is $A = A'A''A''' = 1.3 \times 1.9 \times 1.1 \approx 2.7$. This value is consistent with the observed mismatch between the surface-to-47-m and the surface-to-rock spectral ratios.

Figure 5 also shows that the standard error of the soil-to-rock spectral ratio is conspicuously larger than that of the downhole curve. Roughly, the average uncertainty in an amplification relative to the rock site is 0.25 log units, versus 0.1 in the downhole ratio, corresponding to factors of 1.8 and 1.3, respectively. Thus, the surface-to-rock amplification is a factor of approximately (1.8/1.3) = 1.4 more uncertain, because of the irreducible source and path effects that contribute to it.

In Figure 6a, the fundamental resonance of the upper 17 m of the soil at ~2.2 Hz clearly appears in the weak-motion transfer function (thick line). The soil-to-rock spectral ratio is higher at nearly all frequencies, for the downhole ratio represents only amplification of the upper 17 m. The uncertainties associated with the average soil-to-rock amplification function is again much larger than for the downhole ratio.

Amplification is drastically decreased in strong ground motions, as seen from the downhole curve in Figure 6b (thick line), in full agreement with the nonlinear soil response characteristics (Wen *et al.*, 1994; Beresnev *et al.*, 1995). Nonlinearity eliminates the presence of the resonance peaks outright. Nonlinear response is correctly captured by the soil-to-rock spectral ratios, with the slight overestimate of the "true" response below ~5 Hz.

Comparing Figures 5 and 6, we can assert that the "true" soil amplification given by the uphole/downhole spectral ratios is consistent (within the uncertainties) with the ratio calculated with respect to rock site, if one properly accounts for the limited depth penetrated by the borehole.

Conclusions

The aim of this study is to check the adequacy of the sedimentary site response as characterized by the soil-to-rock spectral ratios that are widely used in engineering seismology practice. We found that this method gives an almost true response at both weak- and strong-motion levels. The apparent departures of the results from the amplification estimated directly from the borehole data are explained by the relatively shallow depth penetrated by the borehole. However, the inherent uncertainties in the soil-to-rock spectral ratios are relatively high due to the finite distance between the stations and the possible distortion of the input signal at rock site. Our conclusions are drawn for the case when stations are 3.3 km apart and the geology is represented by the

alluvial plain deposits in northeastern Taiwan. Nevertheless, these observational conditions are fairly typical.

Acknowledgments

Permission by the Taiwan Power Company (ROC) and the Electric Power Research Institute (USA) to use the unreleased data of the LSST array is gratefully acknowledged. Comments by M. Fehler, G. Atkinson, and an anonymous reviewer are greatly appreciated.

References

Abrahamson, N. A., B. A. Bolt, R. B. Darragh, J. Penzien, and Y. B. Tsai (1987). The SMART 1 accelerograph array (1980–1987), a review, *Earthquake Spectra* **3,** 263–287.

Aki, K. (1993). Local site effects on weak and strong ground motions, *Tectonophysics* **218,** 93–111.

Aki, K. and P. Richards (1980). *Quantitative Seismology. Theory and Methods,* W. H. Freeman and Company, San Francisco.

Beresnev, I. A., K.-L. Wen, and Y. T. Yeh (1995). Seismological evidence for nonlinear elastic ground behavior during large earthquakes, *Soil Dyn. Earthquake Eng.* **14,** 103–114.

Borcherdt, R. D. (1970). Effects of local geology on ground motion near San Francisco Bay, *Bull. Seism. Soc. Am.* **60,** 29–61.

Çelebi, M., J. Prince, C. Dietel, M. Onate, and G. Chavez (1987). The culprit in Mexico City—amplification of motions, *Earthquake Spectra* **3,** 315–328.

Jarpe, S. P., C. H. Cramer, B. E. Tucker, and A. F. Shakal (1988). A comparison of observations of ground response to weak and strong ground motion at Coalinga, California, *Bull. Seism. Soc. Am.* **78,** 421–435.

Murphy, J. R., A. H. Davis, and N. L. Weaver (1971). Amplification of seismic body waves by low-velocity surface layers, *Bull. Seism. Soc. Am.* **61,** 109–145.

Shearer, P. M. and J. A. Orcutt (1987). Surface and near-surface effects on seismic waves—theory and borehole seismometer results, *Bull. Seism. Soc. Am.* **77,** 1168–1196.

Wang, J.-H. (1993). Q values of Taiwan: a review, *J. Geol. Soc. China (Taiwan)* **36,** 15–24.

Wen, K.-L. (1994). Nonlinear soil response in ground motions, *Earthquake Eng. Struct. Dyn.* **23,** 599–608.

Wen, K.-L. and Y. T. Yeh (1984). Seismic velocity structure beneath the SMART1 array, *Bull. Inst. Earth Sci. Academia Sinica* **4,** 51–72.

Wen, K.-L., I. A. Beresnev, and Y. T. Yeh (1994). Nonlinear soil amplification inferred from downhole strong seismic motion data, *Geophys. Res. Lett.* **21,** 2625–2628.

Department of Earth Sciences
Carleton University
1125 Colonel By Drive
Ottawa, Ontario K1S 5B6, Canada
(I.A.B.)

Institute of Earth Sciences
Academia Sinica
P.O. Box 1-55
Nankang, Taipei 11529, Taiwan
(K.-L.W.)

Manuscript received 22 August 1995.